

See discussions, stats, and author profiles for this publication at: <https://www.researchgate.net/publication/324965062>

Field Verification for B-WIM System using Wireless Sensors

Conference Paper · May 2018

DOI: 10.32548/RS.2018.010

CITATIONS

2

READS

70

2 authors:



Yahya M. Mohammed

University of Alabama at Birmingham

8 PUBLICATIONS 14 CITATIONS

SEE PROFILE



Nasim Uddin

University of Alabama at Birmingham

262 PUBLICATIONS 938 CITATIONS

SEE PROFILE

Some of the authors of this publication are also working on these related projects:



Cypher Physical Security NSF-1645863, Uddin (PI): Mobile Automated Rovers Fly-By (MARS-FLY) for Bridge Network Resiliency [View project](#)



NSF-CMMI-533306, Uddin (PI), 10/05-10/13: Multifunctional Composite for Panelized Construction [View project](#)

Field Verification for B-WIM System using Wireless Sensors

Yahya M. Mohammed¹, Nasim Uddin²

¹Research Assistant, Department of Civil Construction and Environmental Engineering, University of Alabama at Birmingham, Birmingham, AL, 35294, USA.

Email: yahya1@uab.edu.

²Ph.D., P.E., Professor, Department of Civil Construction and Environmental Engineering, University of Alabama at Birmingham, Birmingham, AL, 35294, USA.

Email: nuddin@uab.edu.

ABSTRACT

Bridge Weigh-in-Motion (B-WIM) is the concept of using measured strains on a bridge to calculate the static weights of passing traffic loads as they pass overhead at full highway speed. Weight calculations should have a high level of accuracy to enable the B-WIM system from being a tool for direct overload enforcement. This paper describes the experimental testing of the B-WIM system based on moving force identification (MFI) theory. The bridge was instrumented by wireless accelerometers and strain gages attached to the girders to measure the dynamics response when the calibrated trucks pass the bridge. LS-Dyna finite element program is used to imitate the 3-D bridge model, which validated utilizing the collected acceleration data. Then measurements from the wireless strain sensors are utilized to run the (MFI) algorithm and calculate the truck weight.

Keywords: Moving Force Identification (MFI), Bridge Weigh in Motion (B-WIM), Experiment, Verification, 3-D Finite Element Model (3D FEM), Truck weight, Inverse Dynamics;

INTRODUCTION

The American Society of Civil Engineers (ASCE) reported, in the Report Card for America's Infrastructure, that almost four in each 10 bridges are 50 years or older. 56,007 — 9.1% — of America's bridges were structurally deficient in 2016, and on average there were 188 million trips across a structurally deficient bridge each day [1]. In many cases, the current loading on these bridges is significantly different from the service loads at the time of design and construction. To facilitate bridge safety assessment, techniques have been developed to calculate the weights of trucks using the transportation network. Static weighing at weigh stations is accurate but can only provide data for a small sample of passing vehicles [2]. Weigh-in-Motion (WIM) is less accurate but can provide weights for all passing trucks. Bridge Weigh-in-Motion (B-WIM) is one of a number of WIM technologies and accuracies have been reported to be similar to those from other technologies [3].

MFI is the inverse dynamics process of using a structure's response to back-calculate the forces that caused this response. The technique has been used to improve the accuracy of Bridge Weigh-in-Motion (B-WIM) systems. The B-WIM concept is based on Moses's static algorithm [4], which assumes that moving loads will cause bridges to deform in proportion to the sum of products of the axle load magnitudes and the corresponding static influence line ordinates. The advantages of MFI over the traditional static B-WIM methods are that, it can potentially give a complete time history of the wheel forces applied to the bridge, and the errors in B-WIM systems due to bridge dynamics are reduced because the bridge dynamics are accounted for in the new algorithm. Recently, the MFI algorithm has been used to estimate the damage location [5]. The problem of predicting the moving forces in MFI algorithm is formulated as least squares minimization with Tikhonov regularization [6, 7]. The method of Tikhonov regularization [6] addresses ill-conditioning in the equations. It provides a bound to the error and smoother solutions to the MFI problem [8-12]. Dynamic programming with Tikhonov regularization is formulated to solve the inverse structural dynamics problem [13]. Law and Fang [14] have applied the dynamic programming method to the MFI problem using zero order regularization. Then González et al. [15] extended the algorithm with first order regularization of moving forces, which improved the solution accuracy.

MOVING FORCE IDENTIFICATION ALGORITHM

The MFI algorithm uses the inverse dynamics theory to back-calculate a complete time force history of axles or wheels that move on the bridge. The algorithm adopted in this paper is one used by González et al. [15] who

improve the work of Law et al. [14] by applying the first order regularization technique. The algorithm is explained here briefly.

Firstly, the equilibrium equation of motion is converted into a discrete system as shown in Equation (1).

$$[M_g]_{n \times n} \{\ddot{y}\}_{16 \times 1} + [C_g]_{n \times n} \{\dot{y}\}_{n \times 1} + [K_g]_{n \times n} \{y\}_{n \times 1} = [L(t)]_{n \times n_f} \{g(t)\}_{n_f \times 1} \quad (\text{Eq.1})$$

Where M_g , C_g and K_g are the Mass, Damping and stiffness matrices respectively. The terms, \ddot{y} , \dot{y} and y are the acceleration, velocity, and displacements of the DOFs. $L(t)$ is a time varying location matrix used to relate the forces (n_f) of the vector $g(t)$ to the model degrees of freedom (n). The storage requirements of the dynamic programming routine for system of Equations (1) is considerable, especially for a large scale FE model. Therefore, some numerical techniques are necessary to reduce the dimensionality of the system. An eigenvalue reduction technique is employed for this purpose [17]. It is assumed that the displacement vector, $\{y\}$ can be replaced with an equivalent vector of modal coordinates, $\{z\}$, through Equation (2), where $[\Phi]$ is the matrix of normalized eigenvectors and n_z is the number of modes.

$$\{y\} = [\Phi]_{n \times n_z} \{z\}_{n_z \times 1} \quad (\text{Eq.2})$$

Substituting the previous equation into Equation (1) and performing some manipulations, Equation (8) can be written as the decoupled set of equations as expressed by Equation (3).

$$[I]_{n \times n} \{\ddot{z}\} + 2\xi[\Omega]_{n \times n} \{\dot{z}\}_{n \times 1} + [\Omega]_{n \times n} \{z\}_{n \times 1} = [\Phi]^T [L(t)]_{n \times n_f} \{g(t)\}_{n_f \times 1} \quad (\text{Eq.3})$$

Where $[\Omega]$ is a diagonal matrix contains the natural frequencies and ξ is the percentage damping. Equation (3) can now be formulated as a vector matrix differential equation as illustrated in Equation (4).

$$\left\{ \frac{dx}{dt} \right\}_{2n \times 1} = [A]_{2n \times 2n} \{X\}_{2n \times 1} + [B] \{g\}_{n_f \times 1} \quad (\text{Eq.4})$$

Where, $\{X\}_{2n \times 1} = \begin{Bmatrix} z \\ \dot{z} \end{Bmatrix}$, $[A] = \begin{bmatrix} 0 & I \\ -[\Omega] & -2\xi[\Omega] \end{bmatrix}$, $[B] = \begin{bmatrix} 0 \\ [\Phi]^T [L(t)] \end{bmatrix}$

The continuous system of differential equations can be converted into a direct integration scheme, often referred to as a zeroth order system [18] defined by Equations (5,6 and 7).

$$\{X\}_{j+1} = [M] \{X\}_j + [P]_j \{g\}_j \quad (\text{Eq.5})$$

$$[P]_j = [A]^{-1} [M] - [I] \begin{bmatrix} 0 \\ [\Phi]^T [L]_j \end{bmatrix} \quad (\text{Eq.6})$$

$$[M] = \exp([A] * h), \quad h \text{ is the time step} \quad (\text{Eq.7})$$

The second step is applying the least square minimization with Tikhonov regularization parameter as given in Equation (8).

$$\sum_{j=1}^m (\{d_{me}\}_j - [Q] \{X\}_j, [W] \{d_{me}\}_j - [Q] \{X\}_j + \{r\}_j, [B] \{r\}_j) \quad (\text{Eq.8})$$

Where d_{me} is the measurement vector (strain, displacement, or velocity), $[Q]$ is a vector to relate the measurements to the degree of freedom, $\{X\}$ is the degree of freedom vector at each time step j , (x, y) denotes the vector product of x and y , $[W]$ is an $m \times m$ identity matrix in the least squares error. $\{r\}_j$ is the increment change in the force between time step j and time step $j-1$, $[B]$ is a regularized matrix and equal to $\lambda[I]$, where λ is the optimum regularization parameter. This minimization searches for the force increment $\{r\}$ that cause the system best match the given measurements d_{me} . The regularization parameter λ used to avoid the ill-conditioned solution in the previous minimization, also to control the amount of smoothness in force history. The L-curve technique used to calculate the optimal regularization parameter The optimal regularization parameter located at the corner of the L-curve, at the point of maximum curvature [19]. Dynamic programming and Bellman's principle of optimality [13, 19] are used to solve the minimization process.

FIELD TEST OF MFI

Dry Creek Bridge in Bartow County, GA.

The Dry Creek Bridge was built in 2006 and is located on highway SR113 over Dry Creek in Bartow County, Georgia, USA. The bridge has two lanes carrying the eastbound traffic, consists of three simply supported skewed spans. The bridge has five pre-stressed I-shaped concrete girders, a concrete slab, a barrier and both mid- and end-diaphragms. The girders are spaced at 2.67 m intervals and are connected by the slab and the lateral diaphragms. Figure 1 shows the bridge plan and a photograph of the selected span.

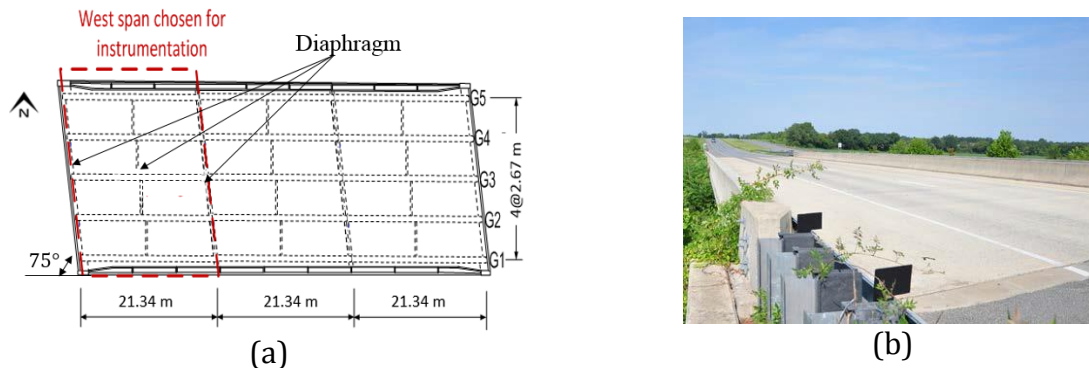


Figure 1. SR113 bridge over Dry Creek: (a) Plan view; (b) Bridge photo.

Bridge instrumentation

The west span among the three is chosen for instrumentation for the B-WIM test. Three types of sensor (accelerometers, strain gages, and displacement transducers), are used to instrument the southwest side of the bridge. The wireless sensing system used in this test is named Martlet [20]. The Martlet wireless node uses a dual-core microcontroller (TMS320F28069) as the processor, featuring up to 90 MHz programmable clock frequency. The 9-channel 12-bit analog-to-digital converter (ADC) allows Martlet to sample analog sensor signals at a rate up to 3 MHz. Only the strain gages at mid-span are used for the MFI study. The sampling frequency of data acquisition system is 200 Hz. Figure 2 shows the instrumentation plan and the elevation for girder G1 and the bridge cross-section.

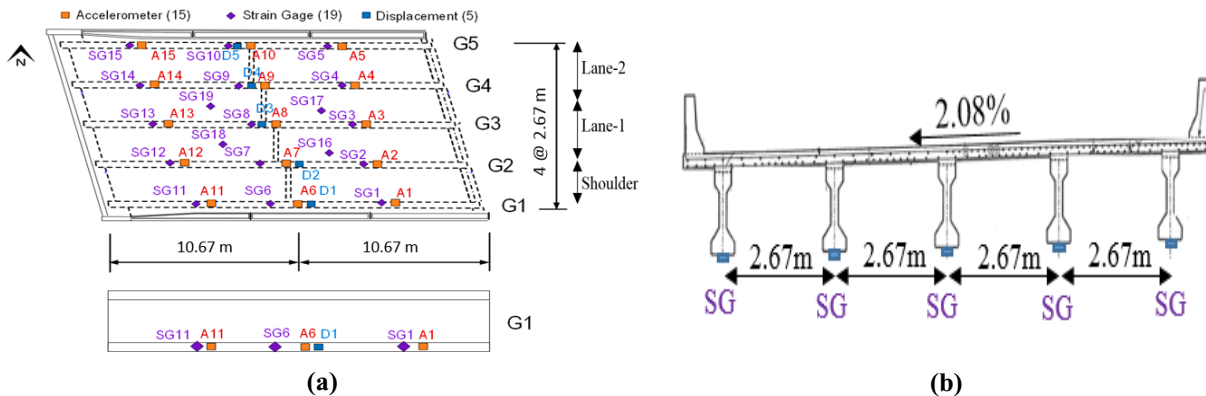


Figure 2. (a) Instrumentation plan on West span and elevation view of girder G1 (b) cross section. (A= accelerometer, SG= strain gage, and D= Displacement).

Test Trucks

Two vehicles manufactured by Navistar International Transportation Corp. (Models 7600 6×4 and 2600 6×4) were adopted for the BWIM validation experiments (Figure 3-a).

Figure 3-b shows the key dimensions of the two vehicles (i.e., distance between axles). Prior to the validation tests, the weight of each vehicle was measured by portable scales

Figure 3-C (Table 1).

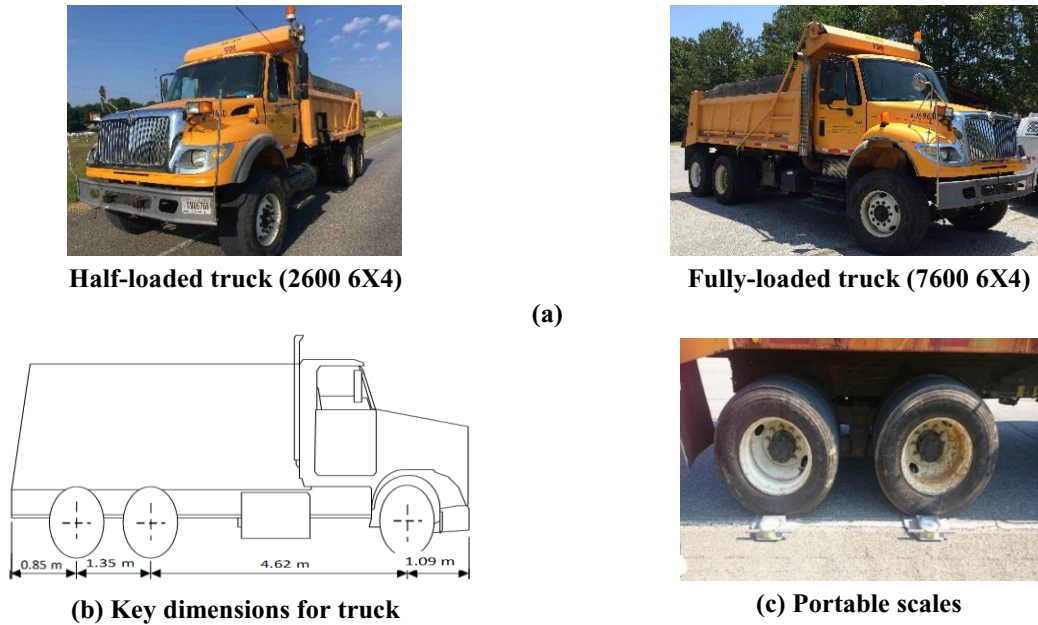


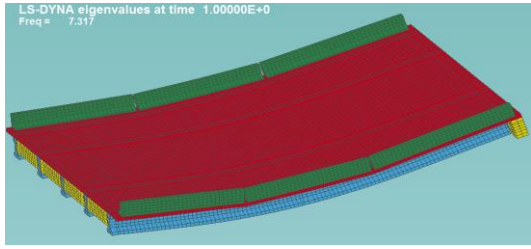
Figure 3. Experiment truck.

Table 1. Vehicle axle weights.

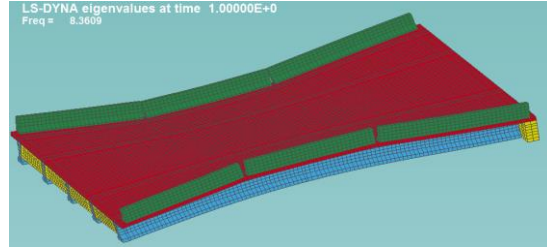
Vehicle number	Weights (kN)			
	Total weight	1st axle	2nd axle	3rd axle
Half-loaded truck	161.5	66.7	48.0	46.8
Fully-loaded truck	201.9	71.8	66.7	63.4

FE Model Calibration.

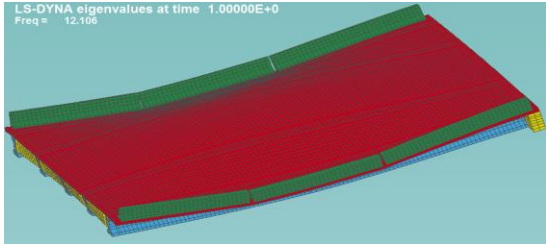
The FE program, LS-Dyna, is utilized to model the bridge. The model was built utilizing solid block elements, with 3 degrees of freedom (DOFs) per node (translation in x, y, and z directions) and 8 nodes. The total number of DOFs for the bridge model is 80,302. The girder acceleration responses from the experiment were analyzed using a Fast Fourier Transform, and the first four frequencies extracted. The Eigenvalue analysis for the bridge model showed that the resonance frequency of the first four modes Figure 4 matched well with the corresponding peak location in the frequency spectra. In addition, Mode 1 shows all five girders bending in one direction, which is expected for this simply supported bridge span. Mode 2 shows opposite bending directions between left (G4, G5) and the right girders (G1, G2).



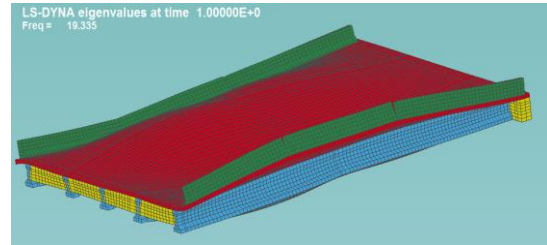
Mode1: f=7.317 HZ



Mode2: f=8.36 HZ



Mode3: f=12.106 HZ



Mode4: f=19.335 HZ

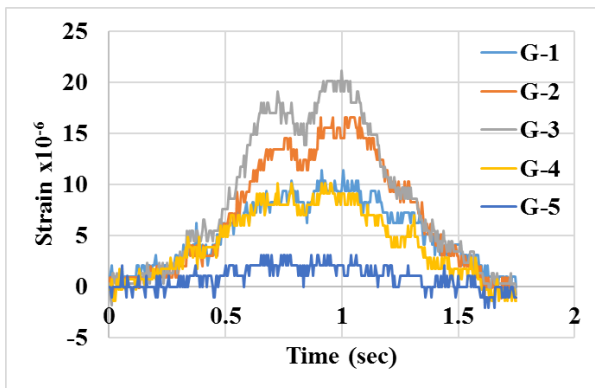
Figure 4. First four natural frequencies of the Georgia, bridge model.

Table 2 provides a comparison between the first four natural frequencies from the experiment and those from the 3-D FE simulation. The 1st natural frequency of the 3-D FEM is lower than the experimental one by 3.2%. The errors in the three other frequencies are all less than 2%.

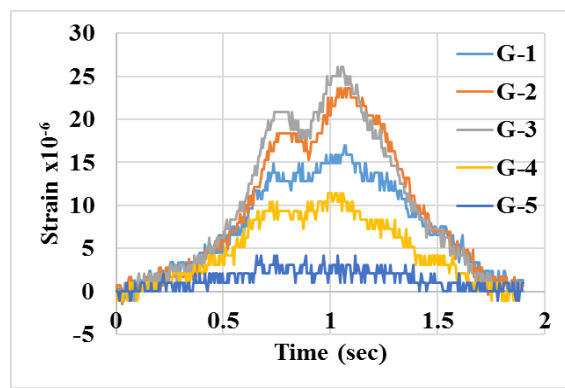
Table 2. Experimental natural frequencies compared with 3-D model ones.

	Experimental natural frequencies	3D model natural frequencies	Error
1st Natural Freq.	7.56 Hz	7.317 HZ	-3.2%
2nd Natural Freq.	8.21 Hz	8.36 HZ	1.83%
3rd Natural Freq.	11.9 Hz	12.10 HZ	1.68%
4th Natural Freq.	19 Hz	19.33 HZ	1.73%

MFI ANALYSIS OF FIELD DATA



(a) Half-loaded truck



(b) Fully-loaded truck

Figure 5. Strain at Girder mid span (G-1= 1st Girder)

In the first two tests, the half and the fully loaded truck traveled on the bridge at a speed of 15.65 m/s and 14.5 m/s respectively. The strains at mid-span of each girders are collected via the wireless strain sensors, and plotted in Figure 5. The number of measurement sensors is five (one for each girder), but each measurement is related to four DOFs (translation in the direction of travel at the four corners of the bottom face of the associated solid element), which translates to 20 measurements. The optimal regularization parameter from the L-curve is found to be 7.42×10^{-15} and 2.02×10^{-15} respectively. The predicted axle force histories for the two trucks are presented in Figure 6 (combining histories for axles of tandems).

Table 3 shows a comparison between the statically measured loads and those predicted. The axle loads are calculated using the average of the middle 60% of the force history [21]. The MFI algorithm detects trucks weight with error less than 5% in the GVW.

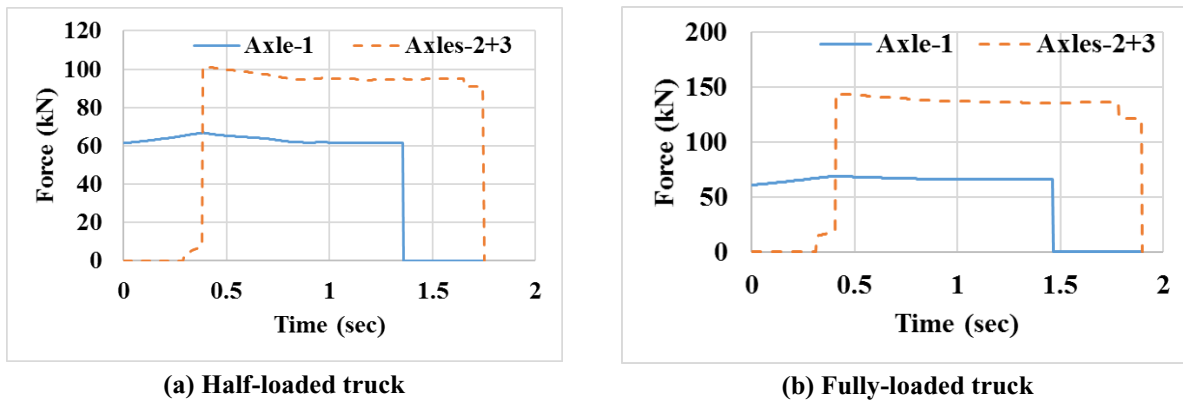


Figure 6. Axles force history.

Table 3. Comparison between the static and the calculated loads.

Item	Half-loaded			Fully-loaded		
	Static weight (kN)	Calculated weight (kN)	Error (%)	Static weight (kN)	Calculated weight (kN)	Error (%)
Axle 1	66.7	63.8	-4.4	71.8	67.9	-5.4
Axles 2+3	94.8	95.2	+0.5	130.2	136.5	+4.8
GVW	161.6	159.0	-1.55	202.0	204.4	+2.2

The experiment has been repeated 3 times with the Half-loaded (H-loaded) truck and one more time with the Full-loaded (F-loaded) one. Table 4 shows the MFI results (GVW)s, and the error percentage for the GVW.

Table 4. Calculated axle loads of H-loaded and F-loaded trucks.

	Truck Type	Speed (m/s)	Axle 1	Axles 2+3	GVW	Error (%)
1	H-loaded	11.0	64.2	97.7	161.9	0.26
2	H-loaded	15.8	65.5	88.2	153.7	-4.8
3	H-loaded	13.15	59.4	100.2	159.6	-1.13
4	F-loaded	15.3	60.9	128.3	189.2	-6.2

CONCLUSION

In conclusion, the moving force identification (MFI) algorithm detected the axles and total weight with high accuracy in most cases. The error in GVWs did not exceeded 5% except the second test for the Fully loaded truck.

The wireless sensors (Marlet) shows the ability to monitor the bridge response and provide the truck weight with acceptable error.

ACKNOWLEDGMENTS

The authors would like to express their gratitude for the financial support received from the National Science Foundation (NSF-CNS- 1645863) for this investigation.

REFERENCES

- [1] ASCE, 2017, "2017 Report card for America's infrastructure," <http://www.infrastructurereportcard.org/>.
- [2] O'Brien, E. J., Znidaric, A., and Dempsey, A. T., 1999, "Comparison of two independently developed bridge weigh-in-motion systems," *International Journal of Heavy Vehicle Systems*, 6(1-4), pp. 147-161.
- [3] Richardson, J., Jones, S., Brown, A., O'Brien, E., and Hajjalizadeh, D., 2014, "On the use of bridge weigh-in-motion for overweight truck enforcement," *International Journal of Heavy Vehicle Systems*, 21(2), pp. 83-104.
- [4] Moses, F., 1979, "Weigh-in-motion system using instrumented bridges," *Journal of Transportation Engineering*, 105:233-249.
- [5] Mohammed, Y. M., and Uddin, N., "Bridge Damage Detection using the Inverse Dynamics Optimization Algorithm," *Proc. 26th ASNT Research Symposium*, pp. 175-184.
- [6] Tikhonov, A. N., Arsenin, V. I. A. k., and John, F., 1977, *Solutions of ill-posed problems*, Winston Washington, DC.
- [7] Neubauer, A., 1989, "Tikhonov regularisation for non-linear ill-posed problems: optimal convergence rates and finite-dimensional approximation," *Inverse problems*, 5(4), p. 541.
- [8] Zhu, X., and Law, S., 2002, "Moving loads identification through regularization," *Journal of engineering mechanics*, 128(9), pp. 989-1000.
- [9] Law, S., Chan, T. H., Zhu, QX, and Zeng, Q., 2001, "Regularization in moving force identification," *Journal of Engineering Mechanics*, 127(2), pp. 136-148.
- [10] Zhu, X., and Law, S., 2003, "Identification of moving interaction forces with incomplete velocity information," *Mechanical systems and signal processing*, 17(6), pp. 1349-1366.
- [11] Zhu, X., and Law, S., 1999, "Moving forces identification on a multi-span continuous bridge," *Journal of sound and vibration*, 228(2), pp. 377-396.
- [12] Law, S., and Zhu, X., 2000, "Study on different beam models in moving force identification," *Journal of sound and vibration*, 234(4), pp. 661-679.
- [13] Trujillo, D., 1978, "Application of dynamic programming to the general inverse problem," *International Journal for Numerical Methods in Engineering*, 12(4), pp. 613-624.
- [14] Law, S., and Fang, Y., 2001, "Moving force identification: optimal state estimation approach," *Journal of Sound and Vibration*, 239(2), pp. 233-254.
- [15] González, A., Rowley, C., and OBrien, E. J., 2008, "A general solution to the identification of moving vehicle forces on a bridge," *International journal for numerical methods in engineering*, 75(3), pp. 335-354.
- [16] !!! INVALID CITATION !!! .
- [17] Busby, H. R., and Trujillo, D. M., 1987, "Solution of an inverse dynamics problem using an eigenvalue reduction technique," *Computers & structures*, 25(1), pp. 109-117.
- [18] Trujillo, D. M., and Busby, H. R., 1997, *Practical inverse analysis in engineering*, CRC Press.
- [19] Hansen, P. C., 1992, "Analysis of discrete ill-posed problems by means of the L-curve," *SIAM review*, 34(4), pp. 561-580.
- [20] Kane, M., Zhu, D., Hirose, M., Dong, X., Winter, B., Häckell, M., Lynch, J. P., Wang, Y., and Swartz, A., "Development of an extensible dual-core wireless sensing node for cyber-physical systems," *Proc. Sensors and Smart Structures Technologies for Civil, Mechanical, and Aerospace Systems 2014*, International Society for Optics and Photonics, p. 90611U.
- [21] Rowley, C. W., 2007, *Moving force identification of axle forces on bridges*, University College Dublin.